Clinical Chemistry 61:3
544–553 (2015)

Clinical Actionability Enhanced through Deep Targeted Sequencing of Solid Tumors

Ken Chen,[1] Funda Meric-Bernstam,[2,3,4] Hao Zhao,[1] Qingxiu Zhang,[3] Nader Ezzeddine,[3] Lin-ya Tang,[3] Yuan Qi,[1] Yong Mao,[1] Tenghui Chen,[1] Zechen Chong,[1] Wanding Zhou,[1] Xiaofeng Zheng,[1] Amber Johnson,[3] Kenneth D. Aldape,[5] Mark J. Routbort,[6] Rajyalakshmi Luthra,[6] Scott Kopetz,[7] Michael A. Davies,[8] John de Groot,[9] Stacy Moulder,[10] Ravi Vinod,[11] Carol J. Farhangfar,[12] Kenna Mills Shaw,[3] John Mendelsohn,[3] Gordon B. Mills,[3,13] and Agda Karina Eterovic[3,13*]

BACKGROUND: Further advances of targeted cancer therapy require comprehensive in-depth profiling of somatic mutations that are present in subpopulations of tumor cells in a clinical tumor sample. However, it is unclear to what extent such intratumor heterogeneity is present and whether it may affect clinical decision-making. To study this question, we established a deep targeted sequencing platform to identify potentially actionable DNA alterations in tumor samples.

METHODS: We assayed 515 formalin-fixed paraffin-embedded (FFPE) tumor samples and matched germline DNA (475 patients) from 11 disease sites by capturing and sequencing all the exons in 201 cancer-related genes. Mutations, indels, and copy number data were reported.

RESULTS: We obtained a 1000-fold mean sequencing depth and identified 4794 nonsynonymous mutations in the samples analyzed, of which 15.2% were present at <10% allele frequency. Most of these low level mutations occurred at known oncogenic hotspots and are likely functional. Identifying low level mutations improved identification of mutations in actionable genes in 118 (24.84%) patients, among which 47 (9.8%) otherwise would have been unactionable. In addition, acquiring ultrahigh depth also ensured a low false discovery rate (<2.2%) from FFPE samples.

CONCLUSIONS: Our results were as accurate as a commercially available CLIA-compliant hotspot panel but allowed the detection of a higher number of mutations in actionable genes. Our study reveals the critical importance of acquiring and utilizing high sequencing depth in profiling clinical tumor samples and presents a very useful platform for implementing routine sequencing in a cancer care institution.

Next generation sequencing can facilitate personalized cancer therapy approaches by identifying actionable somatic events in tumor samples *(1)*. Furthermore, high-quality sequencing data can reveal associations with sensitivity or resistance that can inform the development and implementation of targeted therapeutics and, in particular, aid in the design of future trials to validate findings and actionability. Critical alterations include mutations [single nucleotide variations (SNVs)[14] and insertions and deletions (indels)], copy number variations (CNVs), and rearrangements that can potentially predict response and resistance to targeted agents. Whole genome sequencing (WGS) and whole exome sequencing (WES) allow the detection of SNVs, indels, CNVs, and rearrangements. However, the relatively low coverage of WGS and WES, as currently implemented in most of the sequencing laboratories (100–250×), may have limited ability to cost-effectively detect aberrations that are present in a subpopulation of tumor cells while identifying a myriad of aberrations of unknown clinical significance *(2)*. Somatic aberrations present at low allele frequencies across different types of tumors *(3, 4)* can potentially

[1] Department of Bioinformatics and Computational Biology and [2] Department of Investigational Cancer Therapeutics, The University of Texas MD Anderson Cancer Center, Houston, TX; [3] Institute for Personalized Cancer Therapy, The University of Texas MD Anderson Cancer Center, Houston, TX; [4] Department of Surgical Oncology, [5] Department of Pathology, [6] Department of Hematopathology, [7] Department of GI Medical Oncology, [8] Department of Melanoma Medical Oncology, [9] Department of Neuro Oncology, [10] Department of Breast Medical Oncology, and [11] Department of Sarcoma Medical Oncology, The University of Texas MD Anderson Cancer Center, Houston, TX; [12] Levine Cancer Institute, Carolinas HealthCare System, Charlotte, NC; [13] Department of Systems Biology, MD Anderson Cancer Center, Houston, TX.

* Address correspondence to this author at: The University of Texas MD Anderson Cancer Center, 7777 Knight Rd., Houston, Texas 77054. Fax 713-563-4235; e-mail aketerovic@mdanderson.org.

Received July 29, 2014; accepted December 30, 2014.
Previously published online at DOI: 10.1373/clinchem.2014.231100

[14] Nonstandard abbreviations: SNV, single nucleotide variation; indels, insertions and deletions; CNV, copy number variation; WGS, whole genome sequencing; WES, whole exome sequencing; MAF, mutant allele frequency; FFPE, formalin-fixed paraffin-embedded; COSMIC, Catalogue of Somatic Mutations in Cancer; TCGA, The Cancer Genome Atlas; FDR, false discovery rate; FET, Fisher exact test; H.DEL., highly deleted; H.AMP., highly amplified; ECN, estimated copy number; PCAG, potentially clinically actionable gene; CanDrA, cancer driver annotator; MSI, microsatellite instability.

impact patient prognosis or response *(5)* and thus are important to detect reliably. Targeted sequencing to a depth that allows detection of relatively low mutant allele frequency (MAF) may represent an alternative or a complement to WGS and WES to detect clinically relevant alterations. Additionally, in most clinical and research settings, the amount of DNA that can be isolated from tumor samples is limited and the DNA is often damaged owing to fixation and storage procedures such as those used with formalin-fixed paraffin-embedded (FFPE) samples. Therefore a multiplexed targeted platform that can generate reliable data with high sensitivity from limited amounts of DNA from FFPE samples is needed. Several targeted sequencing panels have been successfully implemented *(6, 7)*. However, the details of a platform's design and parameterization will influence the precision and reliability of the molecular profiling results, impacting both translational research and clinical decision-making. Thus, it is of great value to explore multiple potential solutions in a real patient care environment until a community-wide solution is established, validated, and well accepted.

To identify such a solution, we implemented a deep targeted sequencing platform designed to identify actionable and clinically relevant DNA alterations in 201 cancer-relevant genes (about 5000 exons and 1 Mb of sequence) in clinical samples. Our platform, called T200, was optimized for FFPE samples and low-input DNA. We also optimized the mutation detection approach to reliably detect low-frequency mutations as well CNVs. The data presented here demonstrate the feasibility, challenges, and advantages of a targeted high-depth platform over broader sequencing approaches using clinical samples and its relevance for cancer research and care.

Methods

SELECTION OF THE GENES

We selected 201 genes (see Table 1 in the Data Supplement that accompanies the online version of this report at http://www.clinchem.org/content/vol61/issue3) that are biologically relevant in cancer, on the basis of mutational data in the Catalogue of Somatic Mutations in Cancer (COSMIC) *(8)* and The Cancer Genome Atlas (TCGA). Using those databases, we included genes found mutated in 5% or more of the samples tested across all cancer types (all diseases combined) and in 3% or more of the samples in 1 specific cancer type (e.g., breast cancer) when at least 50 samples had been analyzed. We gave priority to genes or pathways targeted by a drug that was commercially available, in clinical trials, or under late-stage preclinical development. Before implementation of the T200 platform, input on cancer-relevant genes was sought from faculty across The University of Texas MD Anderson Cancer Center. Because depth was important and we desired a panel no larger than 1 Mb, several large genes previously shown mutated i cancer but with no direct clinical implications were not included, such as titin (*TTN*),[15] Wolf-Hirschhorn syndrome candidate 1 (*WGHSC1*, also known as *NSD2*), and microtubule-actin crosslinking factor 1 (*MACF1*). Altogether, the T200 panel comprises 4874 exons encoding 938 607 bases. Our sequencing pipeline consisted of DNA extraction from the sample, library preparation, target enrichment, sequencing, and data analysis (see online Supplemental Fig. 1). Data analysis was optimized for mutation calling from deep coverage (see section 8 of Methods in the online Supplemental Information). Comprehensive details of the study methods are presented in the online Supplemental Information.

Results

RELEVANCE OF SEQUENCING DEPTH AND DNA INPUT

We aimed to determine a minimum sequencing depth at which we were confident in detecting very low–frequency mutations (as low as 1%). Achieving such sensitivity with high confidence is challenging given the degraded nature of FFPE samples and the errors intrinsic to the next generation sequencing *(9, 10)*. According to our power estimation (described in Methods section 6.2 in the online Supplemental Information), about 1000 unique reads are required to ensure detection of 1% frequency alleles with a false discovery rate (FDR) of no

[15] Human genes: *TTN,* titin; *WGHSC1,* Wolf-Hirschhorn syndrome candidate 1 (also known as *NSD2*); *MACF1,* microtubule-actin crosslinking factor 1; *ERBB2,* erb-b2 receptor tyrosine kinase 2; *EGFR,* epidermal growth factor receptor; *HYDIN,* HYDIN, axonemal central pair apparatus protein; *KMT2C,* lysine (K)-specific methyltransferase 2C (also known as *MLL3*); *BRAF,* B-Raf proto-oncogene, serine/threonine kinase; *TP53,* tumor protein p53; *KRAS,* Kirsten rat sarcoma viral oncogene homolog; *NRAS,* neuroblastoma RAS viral (v-ras) oncogene homolog; *PTEN,* phosphatase and tensin homolog; *IDH1,* isocitrate dehydrogenase 1 (NADP+), soluble; *PIK3CA,* phosphatidylinositol-4, 5-bisphosphate 3-kinase, catalytic subunit alpha; *KCNB2,* potassium channel, voltage gated Shab related subfamily B, member 2; *CDKN2A,* cyclin-dependent kinase inhibitor 2A; *NOTCH1,* notch 1; *RB1,* retinoblastoma 1; *CDK4,* cyclin-dependent kinase 4; *FGFR1,* fibroblast growth factor receptor 1; *NF1,* neurofibromin 1; *KIT,* v-kit Hardy-Zuckerman 4 feline sarcoma viral oncogene homolog; *TGFBR2,* transforming growth factor, beta receptor II (70/80kDa); *MSH2,* mutS homolog 2; *MSH6,* mutS homolog 6; *MAP2K4,* mitogen-activated protein kinase kinase 4; *DDR2,* discoidin domain receptor tyrosine kinase 2; *KMT2D,* lysine (K)-specific methyltransferase 2D (also known as *MLL2*); *ERBB4,* erb-b2 receptor tyrosine kinase 4; *SRC,* SRC proto-oncogene, non-receptor tyrosine kinase; *APC,* adenomatous polyposis coli; *MROH2B,* maestro heat-like repeat family member 2B (also known as *HEATR7B2*); *CSMD1,* CUB and Sushi multiple domains 1; *GATA3,* GATA binding protein 3; *ZNF536,* zinc finger protein 536; *GNAQ,* guanine nucleotide binding protein (G protein), q polypeptide; *GNAS,* GNAS complex locus; *PPP1R3A,* protein phosphatase 1, regulatory subunit 3A; *PRSS1,* protease, serine, 1 (trypsin 1); *AR,* androgen receptor; *MECOM,* MDS1 and EVI1 complex locus; *PAPPA2,* pappalysin 2; *CYP2C19,* cytochrome P450, family 2, subfamily C, polypeptide 19; *LPHN3,* latrophilin 3; *HDAC9,* histone deacetylase 9; *PKHD1L1,* polycystic kidney and hepatic disease 1 (autosomal recessive)-like 1; *FAM135B,* family with sequence similarity 135, member B; *EPHA3,* EPH receptor A3; *PCLO,* piccolo presynaptic cytomatrix protein; *PCDH15,* protocadherin-related 15; *CSMD3,* CUB and Sushi multiple domains 3; *SMAD4,* SMAD family member 4; *ATRX,* alpha thalassemia/mental retardation syndrome X-linked; *SMARCA4,* SWI/SNF related, matrix associated, actin dependent regulator of chromatin, subfamily a, member 4.

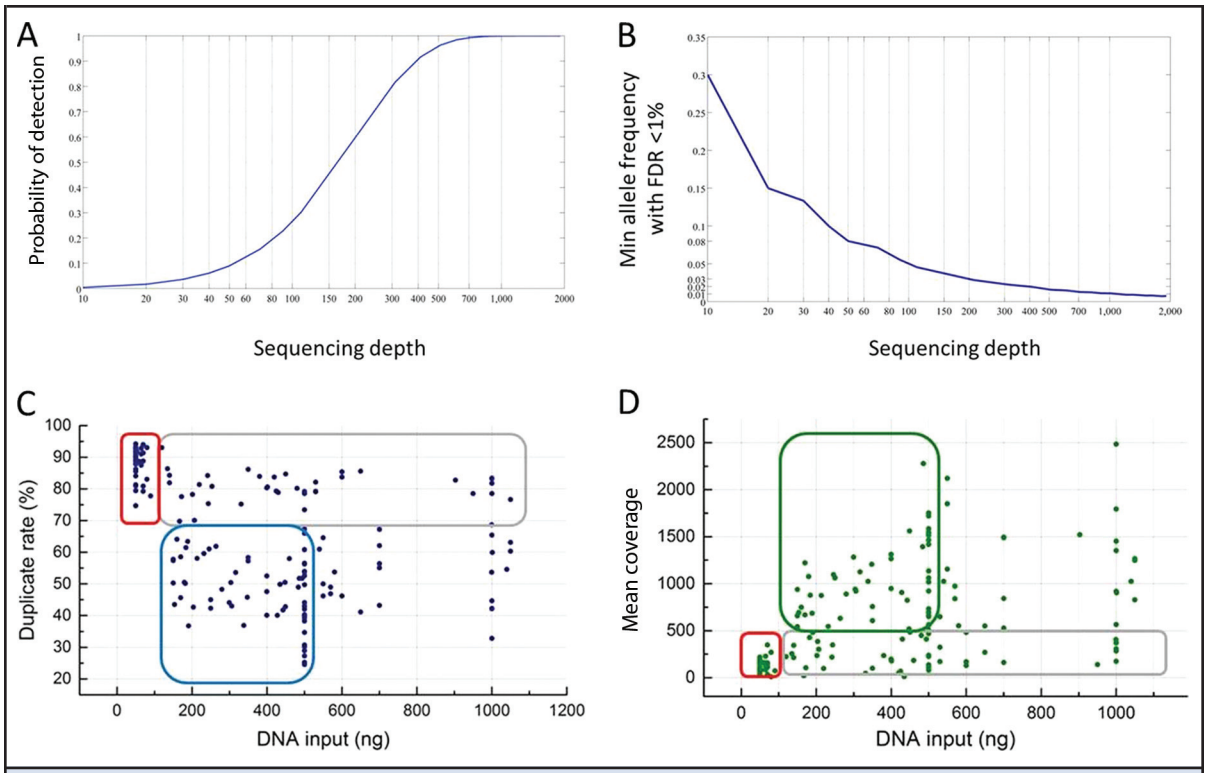

Fig. 1. Technical characterization of T200.

(A), Probability of detecting (i.e., observing 2 or more reads from) a 1% frequency variant allele (*y* axis) from a sequencing coverage (*x* axis) of 10–2000 fold. (B), The minimal (Min) allele frequency (*y* axis) that can be confidently (FDR <1%) detected at a given sequencing coverage (*x* axis). (C, D), DNA input and duplicate rates (C) and depth of coverage (D). Each dot represents 1 tumor sample. Areas circled in red indicate high duplicate rate and low coverage in samples with low DNA input; areas circled in blue and green, ideal range of DNA input to obtain low duplicate rate and desired coverage; areas circled in gray, high duplicate rate and low coverage despite the DNA input.

more than 1% (Fig. 1, A and B). In contrast, at a sequence coverage of 50 reads, the 1% alleles can be detected with merely a 10% chance and with limited confidence (Fig. 1A).

Because the amount of DNA available in clinical settings is limited, we assessed the impact of DNA input in the coverage. We established a minimum of 170 ng of DNA input for our pipeline, although we were able to generate data with as little as 50 ng. This cutoff was established on the basis of our data from FFPE clinical samples showing that <170 ng of DNA drastically increased the duplicate rate, consequently decreasing sequencing depth (Fig. 1, C and D, respectively). Furthermore, with <100 ng of input DNA, the duplicate rate was higher than 70%, whereas the highest coverage achieved was 347× (red rectangles in Fig. 1, C and D), which would make it impossible to call 1% frequency mutations from 15% of target sites (according to Fig. 1A). Interestingly, our data shows that DNA input higher than 500 ng did not necessarily improve the performance in terms of either duplicate rate or coverage. Therefore, the ideal range for DNA input on this platform was between 170 and 500 ng (blue and green rectangles in Fig. 1, C and D). Samples highlighted in gray rectangles showed high duplicate rate (Fig. 1C) and low depth (Fig. 1D) despite the amount of DNA input, which was probably an effect of different levels of DNA damage in the FFPE sample pool.

PLATFORM PERFORMANCE, SENSITIVITY, AND SPECIFICITY

Because most of the tumor samples in our institution and many others around the world are FFPE derived, it was important to ensure that our platform was prepared to handle this type of material, despite the DNA damage that the fixation process introduces *(10)*. To test the robustness of the T200 pipeline in FFPE samples, we sequenced a pair of matched fresh-frozen and FFPE tumor samples and compared the variant allele frequencies estimated for them. We found high concordances between the fresh-frozen and FFPE tissues in sites with more than 200 reads ($r^2 \geq 0.92$, Fig. 2A and B). For sites with fewer than 200 reads, the correlation between fresh-

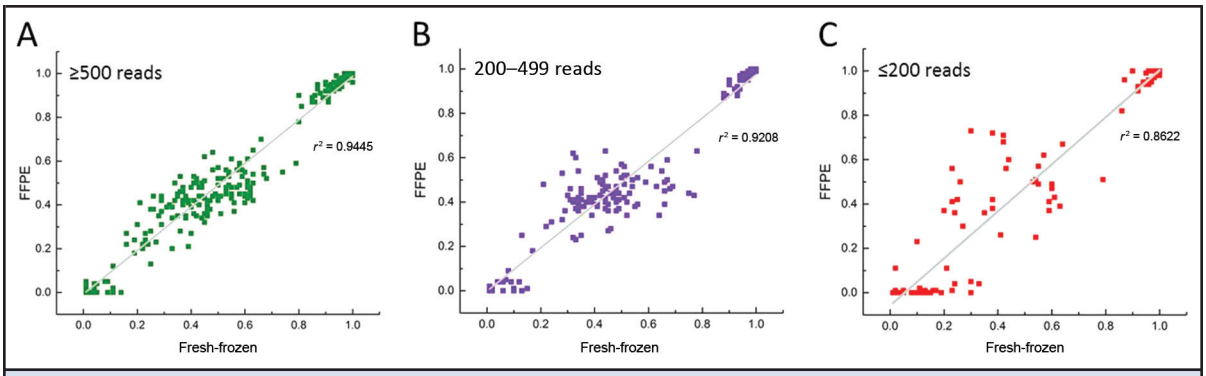

Fig. 2. Concordance between fresh-frozen and FFPE samples.

Each dot represents an SNV in a matched pair of fresh-frozen and FFPE tumor samples detected at above 500 reads (high correlation) (A), between 200 and 499 reads (medium to high correlation) (B), and below 200 reads (low correlation) (C).

frozen and paraffin decreased markedly, with $r^2 = 0.86$ (Fig. 2C). Another pair of matched fresh-frozen-FFPE pairs was independently processed, captured, and sequenced and showed similar results (see online Supplemental Fig. 2), demonstrating the reproducibility of our platform.

We also examined the accuracy of copy number prediction using our platform. We compared the erb-b2 receptor tyrosine kinase 2 (*ERBB2*) (Her2) copy number status measured in tumor samples by the T200 platform with those obtained from FISH (fluorescent in situ hybridization) or immunohistochemistry for the same samples. We found an accurate (98.3%) classification rate for the high copy number (≥5) amplifications (see online Supplemental Fig. 3). In addition, the high depth allowed robust detection of focal alterations, as demonstrated by a sharp dip in read counts across exons removed by a homozygous epidermal growth factor receptor (*EGFR*) vIII deletion in a brain and a breast cancer sample (see online Supplemental Fig. 4). We also validated the copy number data for 6 breast cancer samples using the Oncoscan copy number platform from Affymetrix. Our level of concordance for highly deleted (H.DEL.) was 100% for 5 of the samples analyzed. For highly amplified (H.AMP.), We found 100% of concordance for 4 out of 6 samples (see online Supplemental Table 2).

DETECTION OF GENOMIC ALTERATIONS IN CLINICALLY ACTIONABLE GENES IN FFPE TUMOR SAMPLES

In this study we defined genes as potentially actionable if alterations in the gene may potentially direct treatment options from: (*a*) the availability of approved drugs that directly or indirectly target the gene, (*b*) predicted resistance to existing treatment options, and/or (*c*) clinical trials selecting for genomic alterations in the gene of interest. On the basis of this rationale, there were 112 actionable genes in the T200 panel (see online Supplemental Table 3).

Depth of coverage in clinical samples. We analyzed 515 tumors (all FFPE) and matched normal (blood) samples of 475 patients in 11 disease sites: breast (22%), skin (20%), brain (16%), colon (15%), and sarcoma (9%), as well as ovarian, stomach, kidney, head and neck, lung and prostate (3% or less; Fig. 3A). After mapping and removing duplicate reads, we obtained a median average haploid coverage of 906× on the targeted region of the tumors (Fig. 3B). The median coverage appeared to be consistent in the majority of targeted exons (≥200× and ≤1400× in ≥98.2% of the exons; see online Supplemental Fig. 5A). Not surprisingly, the exons with extremely low coverage (<200×) reside in GC-rich (>70%) regions which are difficult to amplify and sequence (see online Supplemental Fig. 5, B and C). Most of the exons with extremely high coverage (>1400×) appeared to come from a few genes [HYDIN, axonemal central pair apparatus protein (*HYDIN*) and lysine (K)-specific methyltransferase 2C (*KMT2C*, also known as *MLL3*)] and were likely caused by incompleteness (homologous regions not represented) in the hg19 reference genome (see online Supplemental Table 4); we therefore excluded mutations detected in those exons. Overall, 98.7% of target sites had at least 200-fold coverage (Fig. 3C) and 87.6% had at least 500-fold coverage (not shown).

Detection of somatic mutations and copy number alterations. We found 4794 nonsynonymous somatic mutations (including 4525 SNVs and 269 indels) from 515 tumor samples, with a median mutation rate of 1 per Mb in sarcoma, 3 in breast, ovarian and brain cancers, 6 in colorectal cancer, and 17 in skin cancer (Fig. 3D). No nonsynonymous somatic mutations in the 201 genes

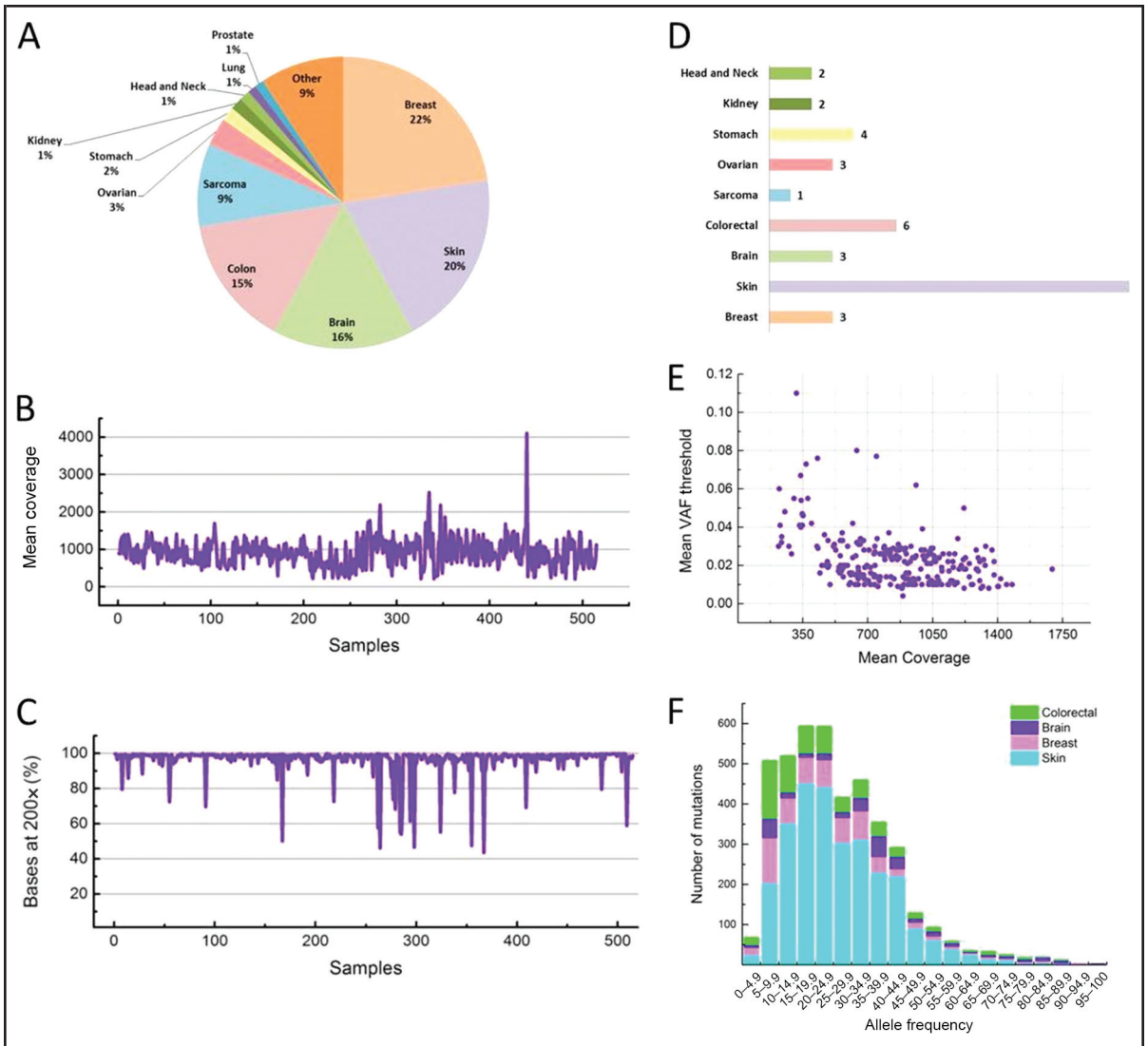

Fig. 3. Mutation profiling of 515 tumor samples using T200.

(A), Distribution of disease sites; (B), mean coverage (*y* axis) in each sample (*x* axis, in no particular order); (C), percentage of target bases (*y* axis) that are covered by at least 200× in each sample (*x* axis in no particular order); (D), median mutation rate (per Mb) in 9 major (>10 samples) cancer types; (E), the mean variant allele frequency cutoff (*y* axis) applied in variant calling as a function of mean coverage (*x* axis) in each sample; and (F), number of mutations (*y* axis) detected in various allele frequency bins (*x* axis) for 4 cancer types.

were found in 25 (5%) of the tumors pairs. The uniformly deep coverage across exons allowed sensitive and accurate detection of mutations with MAF as low as 1% at most of the target sites. To achieve a low false-discovery rate (around 1%), we applied stringent MAF cutoffs on our calls, which averaged from 0.4% to 11% with a median of 2.1% (Fig. 3E). We found 730 (15.23%) low-frequency (<10% MAF) mutations. Among those, 98 (13.4%) were found in the COSMIC, which is similar [$P \geq 0.22$, Fisher exact test (FET)] to the percentage 632/4064 (15.6%) of mutations found in COSMIC among high-frequency (≥10% MAF) mutations.

The low-frequency mutation landscape was similar to that of high-frequency mutations. For example, 6 of 7 low-frequency B-Raf proto-oncogene, serine/threonine kinase (*BRAF*) mutations occurred at amino acid position 600 and the seventh occurred at position 594 (not shown). Overall, similar total numbers of mutations were detected between 5%–10%, 10%–15%, 15%–20%, and 20%–25% MAF (Fig. 3F). In comparison mutations

found in skin tumors, more mutations were found between 5% and 10% MAF in breast ($P < 5.7e-9$, FET), brain ($P < 2.8e-8$, FET), and colorectal ($P < 2.5e-12$, FET) tumors, indicating a potentially higher degree of intratumor heterogeneity or contaminating normal tissue cells in these tumor types.

We identified 35 significantly mutated genes that we defined as those that harbored significantly more nonsynonymous mutations than expected by chance from their exon sizes ($P < 0.01$, Poisson test, FDR corrected; see online Supplemental Table 5). At the top of the significantly mutated genes list were well-known driver genes tumor protein p53 (*TP53*), Kirsten rat sarcoma viral oncogene homolog (*KRAS*), *BRAF*, neuroblastoma RAS viral (v-ras) oncogene homolog (*NRAS*), phosphatase and tensin homolog (*PTEN*), isocitrate dehydrogenase 1 (NADP+), soluble (*IDH1*), phosphatidylinositol-4,5-bisphosphate 3-kinase, catalytic subunit alpha (*PIK3CA*), potassium channel, voltage gated Shab related subfamily B, member 2 (*KCNB2*), cyclin-dependent kinase inhibitor 2A (*CDKN2A*), and *EGFR*, which previously have been shown to be significantly mutated in cancer *(11, 12)*. In our analysis, many genes were significantly mutated only in specific tumor types such as *BRAF* and *NRAS* in skin, *IDH1* and *EGFR* in brain, and *PIK3CA* in breast cancer. These data well recapitulated previous cancer genomics studies *(11–13)* (Fig. 4).

We found at least 1 H.AMP or H.DEL gene in 175 (34.0%) tumor samples. We defined a gene as H.AMP if its estimated copy number (ECN) was ≥5. We defined a gene as H.DEL if its ECN was ≤0.6. From these, we derived a list of 30 genes with significant copy-number alterations ($P < 0.01$, Poisson test, FDR corrected; see online Supplemental Table 6). The majority of these genes [including notch 1 (*NOTCH1*), *EGFR*, retinoblastoma 1 (*RB1*), *PTEN*, cyclin-dependent kinase 4 (*CDK4*), *ERBB2*, fibroblast growth factor receptor 1 (*FGFR1*), *TP53*, neurofibromin 1 (*NF1*), and v-kit Hardy-Zuckerman 4 feline sarcoma viral oncogene homolog (*KIT*)] were known to have significantly altered copy numbers in cancer *(14)*. Tumor suppressor genes such as *RB1*, *PTEN*, *TP53,* and *NF1* were frequently deleted, and oncogenes including *EGFR, CDK4*, *ERBB1*, *FGFR1*, and *KIT* were frequently amplified. Like the genes with nonsynonymous mutations, these genes were altered in a cancer-type–specific fashion. For example, *EGFR* was significantly amplified only in brain, whereas *RB1* was significantly deleted only in sarcoma.

Three hundred nineteen of the 475 patients (67%) assessed had high-frequency aberrations in at least 1 potentially clinically actionable gene (PCAG) (see online Supplemental Table 3) and 118 (24.84%) patients had low-frequency mutations in PCAGs. Forty-seven (9.8%) patients had only low-frequency mutations in PCAGs. Overall 336 (70.73%) patients had nonsynonymous mutations in at least 1 PCAG. In addition to SNVs and indels, we also found that 155 (32.63%) patients had high copy number alterations in at least 1 PCAG. Taking both mutations and CNVs into account, we found alterations in at least 1 PCAG in 387 (81.47%) of the 475 patients using T200.

The identified nonsynonymous mutations appeared to affect the function of PCAGs in a variety of ways (see online Supplemental Table 7). Most were missense mutations that may not be functional. To obtain more precise characterization, we developed a cancer driver annotator (CanDrA) *(15)*, which estimates the likelihood that a missense SNV in a given cancer type is a driver based on a large set of evidence summarizing aspects of sequence conservation, protein structure, sequence context, mutational spectrum, and mutation prevalence (96 features) in the COSMIC, TCGA and CCLE (Cancer Cell Line Encyclopedia) *(16)* databases. We annotated each missense SNV in our set as either functional or nonfunctional using CanDrA, in conjunction with Mutation Assessor, SIFT (Sorts Intolerant From Tolerant substitutions), PolyPhen, and ConDel among others *(17)*. When we excluded SNVs that were annotated as nonfunctional by any of these annotators, 216 (45.47%) patients had potential functional mutations in at least 1 PCAG (see Supplemental Table 8). Among these patients, 60 (27.8%) had low-frequency functional mutations; 77 (35.6%) had 2 or more potentially functional mutations, which may pose both opportunities and challenges for clinical decision-making.

Among the 475 patients, 25 had both primary and metastatic tumors sequenced. Although derived from the same patients, these tumor samples may differ considerably owing to tumor evolution *(3)*. Nonetheless, 548 (78.4%) of the 699 of mutations in the metastasis samples were present in the corresponding primary tumors. This result not only demonstrated the reproducibility of our assay but also suggested that clonal heterogeneity may be developed in only a subset of patients. Indeed, more than half (89/151) of nonrecurring mutations were found in 15 tumor samples derived from 8 patients with colorectal cancer. Among them, at least 4 primary-metastasis pairs from different patients demonstrated a microsatellite instability (MSI) phenotype with high mutation rates (7–48 mutations per Mb) and harbored functional somatic mutations in transforming growth factor, beta receptor II (70/80kDa) (*TGFBR2*) and *BRAF* which are suggestive of MSI or germline deleterious mutations in the mismatch-repairing genes mutS homolog 2 (*MSH2*) and mutS homolog 6 (*MSH6*) *(18, 19)* (not shown). Mutations in these samples clustered at different allele frequencies (3 pairs shown in online Supplemental Fig. 6). Unlike previous studies *(3, 20)*, in this study we could confidently identify mutation clustering, around

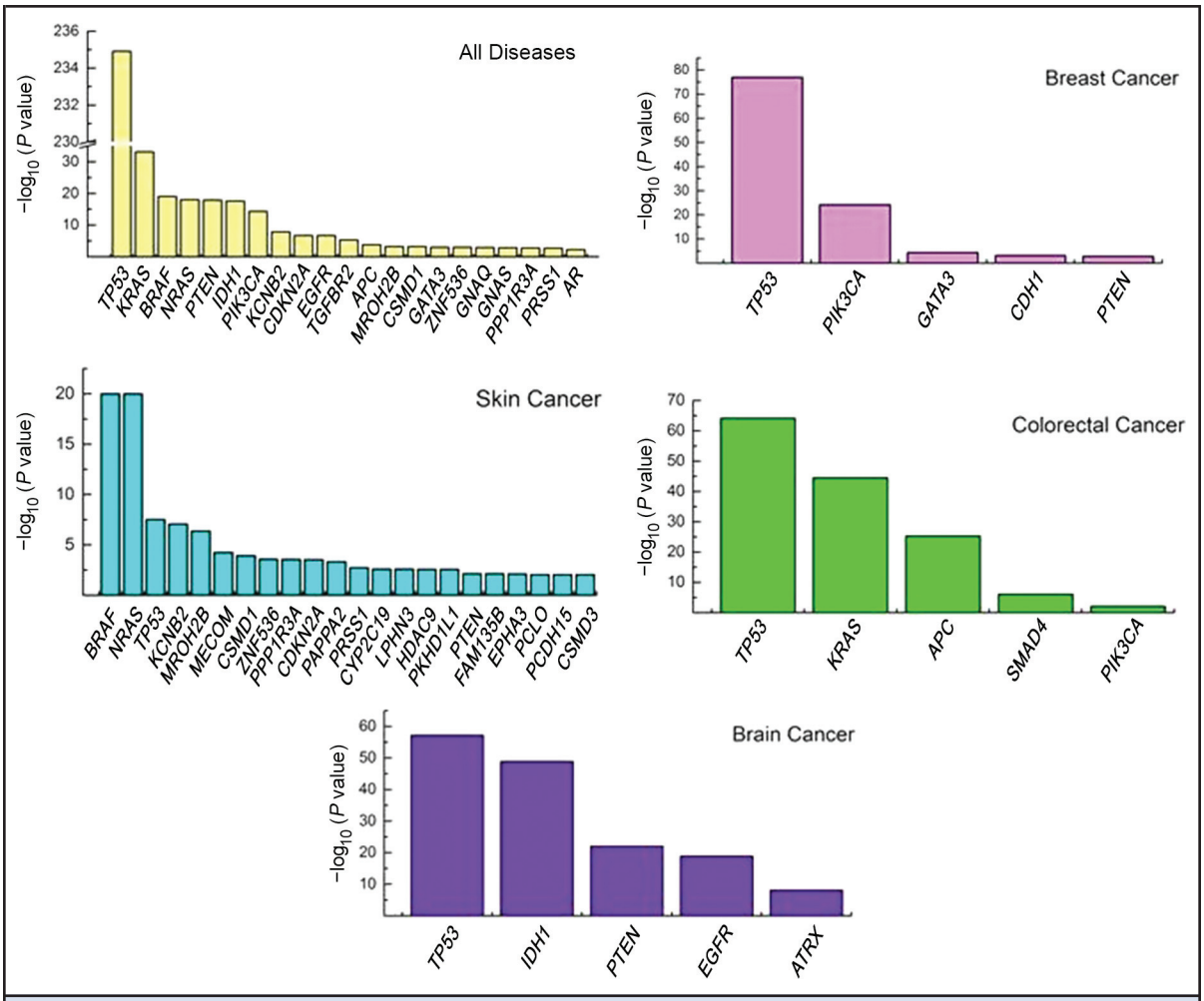

Fig. 4. Significantly mutated genes.

Negative $\log_{10}$ *P* values (*y* axis) of significantly mutated genes (*x* axis) in 5 disease categories: all diseases and breast, skin, colorectal and brain cancers. *APC,* adenomatous polyposis coli; *MROH2B,* maestro heat-like repeat family member 2B (also known as *HEATR7B2*); *CSMD1,* CUB and Sushi multiple domains 1; *GATA3,* GATA binding protein 3; *ZNF536,* zinc finger protein 536; *GNAQ,* guanine nucleotide binding protein (G protein), q polypeptide; *GNAS,* GNAS complex locus; *PPP1R3A,* protein phosphatase 1, regulatory subunit 3A; *PRSS1,* protease, serine, 1 (trypsin 1); *AR,* androgen receptor; *MECOM,* MDS1 and EVI1 complex locus; *PAPPA2,* pappalysin 2; *CYP2C19,* cytochrome P450, family 2, subfamily C, polypeptide 19; *LPHN3,* latrophilin 3; *HDAC9,* histone deacetylase 9; *PKHD1L1,* polycystic kidney and hepatic disease 1 (autosomal recessive)-like 1; *FAM135B,* family with sequence similarity 135, member B; *EPHA3,* EPH receptor A3; *PCLO,* piccolo presynaptic cytomatrix protein; *PCDH15,* protocadherin-related 15; *CSMD3,* CUB and Sushi multiple domains 3; *SMAD4,* SMAD family member 4; *ATRX,* alpha thalassemia/mental retardation syndrome X-linked.

5% allele frequencies, although we sequenced the exons of only 201 genes. Some of these low-frequency mutations were found in important cancer genes such as mitogen-activated protein kinase 4 (*MAP2K4*), discoidin domain receptor tyrosine kinase 2 (*DDR2*), and lysine (K)-specific methyltransferase 2D (*KMT2D*, also known as *MLL2*) (see online Supplemental Fig. 6, A and B). A nonsense mutation *APC* E1309* was detected at a mere 2.33% allele frequency (see online Supplemental Fig. 6C). All of the frameshift mutations in *TGFBR2* occurred at low frequency, suggesting the presence of MSI subclones in these tumors. Overall, significantly more nonrecurring mutations (61/151 vs 29/548, $P < 2.2e\text{-}16$, FET) were in lower frequency than recurring mutations, suggesting that a subgroup of the nonrecurring mutations may be present in both the primary and the metastasis but was below the sensitivity of detection at that allele in either sample.

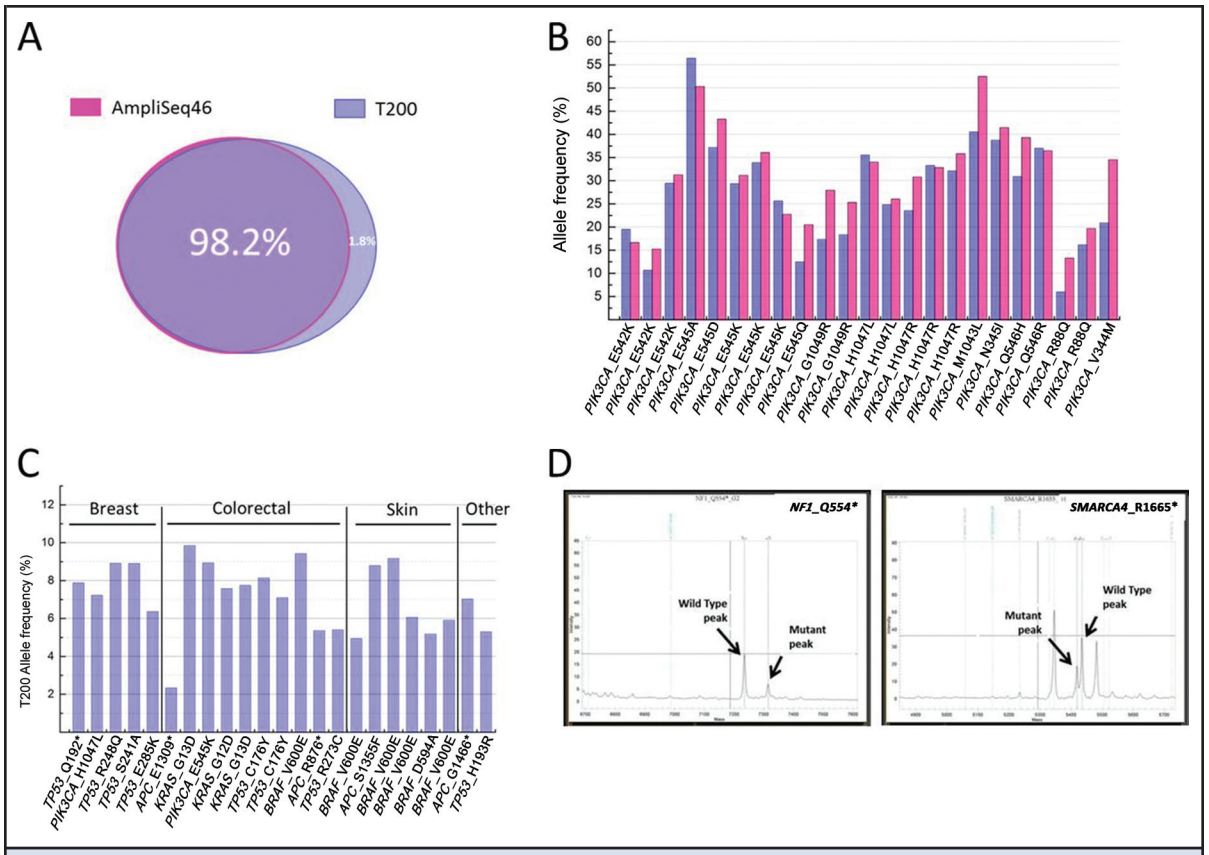

Fig. 5. Concordance with other sequencing platforms.

All the samples tested in this study were also tested in the AmpliSeq46 gene panel in a CLIA-accredited clinical laboratory. (A), 98.2% of mutations identified by AmpliSeq46 were also identified by T200. (B), Allele frequency of *PIK3CA* mutations identified in different patients by AmpliSeq46 (pink bars) and T200 (blue bars). (C), Mutations found at lower than 10% MAF by T200 in different cancer types validated by AmpliSeq46. (D) Peaks obtained from Sequenom validation of 2 new mutations identified by T200 (*NF1*_Q554* and *SMARCA4*_R1665*). A complete list of all sites tested on Sequenom can be found in the online Supplemental Data. *, Stop codon; *SMARCA4,* SWI/SNF related, matrix associated, actin dependent regulator of chromatin, subfamily a, member 4.

CONCORDANCE WITH OTHER SEQUENCING PLATFORMS

Validation of next generation sequencing data is critical, especially when this technology is used to screen. All the samples tested in this study were tested on the AmpliSeq46 gene panel in a CLIA-accredited clinical laboratory at The University of Texas MD Anderson Cancer Center *(21)*. The AmpliSeq46 was designed by Ion Torrent (Life Technologies) and it is an amplicon-based panel of 46 cancer-related genes (see online Supplemental Table 9). All the genes in this panel except erb-b2 receptor tyrosine kinase 4 (*ERBB4*) and SRC proto-oncogene, non-receptor tyrosine kinase (*SRC*) are also in the T200 gene panel. We found that 98.2% of mutations identified by CMS46 were also identified by T200 (Fig. 5A). It is important to mention that the DNA samples used in both platforms (T200 and AmpliSeq46) were extracted from different batches of slides from the same paraffin block for each patient. We also compared the MAFs for the most common *PIK3CA* mutations detected by both sequencing platforms and found similar frequencies for the sites compared (Fig. 5B). Mutations found at lower than 10% MAF and identified by both platforms are represented in Fig. 5C, showing the reliability of the T200 platform to detect the low-frequency mutations.

To estimate the false discovery rate of T200, we randomly selected 98 novel T200 mutations that were not covered by the AmpliSeq46 platform, not found in the COSMIC v63, and had allele frequencies >10%. We retested them using Sequenom MassArray™ (see online Supplemental Table 10). Out of the 98 new sites tested, 96 were validated, which indicated a 2.0% false discovery rate. The wild-type and mutant peaks for 2 of the sites tested and validated are shown in Fig. 5D.

Discussion

Our study describes a newly developed targeted DNA sequencing platform to screen 201 genes (all exons) in tumor DNA samples. The platform is suitable to be implemented in clinical settings and can greatly contribute to the tailoring of cancer treatment to specific patients.

We first evaluated the effects of sequencing depth and DNA input on the sensitivity of our platform. Our data clearly showed that although we could obtain data from as low as 50 ng of input genomic DNA, amounts <100 ng significantly increased the duplicate rate, consequently decreasing the depth–probably owing to the limited library diversity–and thus limiting our ability to call rare events. Importantly, although we had access to only 2 to 4 FFPE slides for most of the patients, only a small percentage of patients (<5%) did not have enough DNA for sequencing. Furthermore, despite the relatively low input and the degraded nature of the FFPE DNA, our failure rate, defined by <10 median nonredundant reads, was lower than 2%.

Another goal of our study was to compare fresh-frozen and matched FFPE samples and assess how the depth of sequencing could impact the performance of more challenging samples such as FFPE. The correlation between MAF in fresh-frozen and matched paraffin samples was expressively high at medium and high depth but was significantly lower at sequencing depths lower than 200×. Thus, using approaches that do not routinely reach the required depth for FFPE samples can be challenging and may be risky regarding mutation identification. Importantly, the difference between assessment of paraffin and fresh-frozen samples, which by necessity are from different parts of the tumor, may represent intratumoral heterogeneity. However, at least in these cases, very little intratumoral heterogeneity in this set of cancer genes was present (maximum of 3%).

We then sequenced 515 tumor samples and their matched normal samples across several disease sites. The average coverage with our platform was higher than 900×, with some regions having lower coverage, most of which were found to be CG enriched. The mutational landscape revealed across the disease sites was similar to those found by other large sequencing databases such as TCGA, demonstrating the robustness and reliability of the T200 platform. Our data also show that this platform can identify potential subclones and heterogeneity between primary and metastatic samples. Additionally, the fact that the low-frequency mutation landscape was similar to those of high-frequency mutations suggests that the low-frequency mutations are unlikely false positives and reinforces the importance of a high-depth sequencing platform. In our study, the deep coverage enabled sensitive discovery of mutations in as low as 1% MAF, which would be important either when tumor content is low or when tumors are heterogeneous. Consequently, we were able to detect mutations in potentially clinically actionable genes in 81.5% of patients, which was substantially more than the percentage of patients with mutations in actionable genes based on a CLIA-compliant hotspot assay (AmpliSeq46) (not shown). However it should be emphasized that many of the alterations identified with T200 were missense mutations with unknown biological and clinical implications; thus not all mutations in actionable genes may be clinically actionable.

Although our results were obtained in a preclinical research environment, through an institutional review board–approved protocol, they were used to guide clinical decision-making. All the T200 results were returned to treating physicians, who were able to order additional CLIA-compliant assays to confirm alterations that were relevant for decision-making. Notably, the reported prospective laboratory protocol was focused on discovery of somatic alterations. However, our sequencing of matched germline DNA not only made it possible to reliably distinguish somatic and germline mutations, but also enabled us to uncover pathogenic germline mutations that may indicate the potential risks for and heritability of a wide spectrum of genetic diseases, so-called "incidental findings" *(22)*. Therefore, a companion germline analysis protocol with prospective informed consent has been activated to facilitate discovery of germline alterations and to solicit patient preferences of return of incidental results. Germline variant annotation algorithms have just been established and identification and validation of deleterious findings is still ongoing.

The deep coverage ensured a very low false-discovery rate (<2%), as validated by our side-by-side comparison of our results with results obtained from multiple orthogonal assays. Therefore, these highly accurate results could be routinely obtained in important cancer genes from FFPE tumor samples at a reasonable cost. Although a smaller panel of known mutations based on specific cancer types could be an alternative to T200, our platform can potentially identify new unexpected genomic aberrations in specific disease sites which can potentially lead to the development of new clinical trials or increase the enrollment of patients in existing ones.

Our study also revealed a few limitations of T200. One of the main limitations is the turnaround time. The current turnaround time of T200 is 3–4 weeks in the best case scenario, which is not ideal in a clinical environment and needs further improvement. Another limitation is that, as with any other targeted panel, we could not identify mutations outside of our target region. This limitation can be improved by routinely updating the panel on the basis of new discoveries from inside and outside our group, such as those from recent large-scale pan-cancer studies *(11, 12, 14)* and studies of unusual responders and markers of sensitivity and resistance. We

are now in the process of updating our T200 platform by adding new potentially actionable genes and a whole genome copy number scan to allow analysis of regional copy number changes while keeping the panel at no more than 2 Mb to achieve the coverage desired and without dramatically inflating costs.

Taken together, the advantages of targeted exome sequencing in sensitivity, clinical relevance, robustness, and cost outweigh its limitations and have made it one of the most promising approaches for clinical cancer genomic profiling. The aspects emphasized here seem to be crucially important in clinical scenarios and should be taken in consideration when making treatment decisions based on sequencing data.

Author Contributions: *All authors confirmed they have contributed to the intellectual content of this paper and have met the following 3 requirements: (a) significant contributions to the conception and design, acquisition of data, or analysis and interpretation of data; (b) drafting or revising the article for intellectual content; and (c) final approval of the published article.*

Authors' Disclosures or Potential Conflicts of Interest: *Upon manuscript submission, all authors completed the author disclosure form. Disclosures and/or potential conflicts of interest:*

Employment or Leadership: Q. Zhang, UT MD Anderson Cancer Center; N. Ezzeddine, UT MD Anderson Cancer Center.
Consultant or Advisory Role: J. de Groot, Glaxosmithkline, Genentech, Novartis, and Sanofi-Aventis; G.B. Mills, Illumina, AstraZeneca, Blend, Critical Outcome Technologies, HanAl Bio Korea, Nuevolution, Pfizer, Provista Diagnostics, Roche, Signalchem Lifesciences, Symphogen, and Tau Therapeutics.
Stock Ownership: None declared.
Honoraria: None declared.
Research Funding: The Sheikh Bin Zayed Al Nahyan Foundation (1U01 CA180964), NCATS grant UL1 TR000371 (Center for Clinical and Translational Sciences), the Bosarge Foundation, the MD Anderson Cancer Center Support grant (NIH/NCI P30 CA016672), and the MD Anderson Moon Shot Program; K. Chen, NCI R01 CA172652; K.M. Shaw, institutional funding from the Khalifa Foundation; M.A. Davies, NIH 1R01CA172670.
Expert Testimony: None declared.
Patents: None declared.

Role of Sponsor: The funding organizations played no role in the design of study, choice of enrolled patients, review and interpretation of data, or preparation or approval of manuscript.

Acknowledgments: We thank Sarah J. Bronson from the MD Anderson Scientific Publications Department for reviewing this manuscript.

References

1. Roychowdhury S, Iyer MK, Robinson DR, Lonigro RJ, Wu YM, Cao X, et al. Personalized oncology through integrative high-throughput sequencing: a pilot study. Sci Transl Med 2011;3:111ra21.
2. Vogelstein B, Papadopoulos N, Velculescu VE, Zhou S, Diaz LA Jr, Kinzler KW. Cancer genome landscapes. Science 2013;339:1546–58.
3. Ding L, Ley TJ, Larson DE, Miller CA, Koboldt DC, Welch JS, et al. Clonal evolution in relapsed acute myeloid leukaemia revealed by whole-genome sequencing. Nature 2012;481:506–10.
4. Shah SP, Roth A, Goya R, Oloumi A, Ha G, Zhao Y, et al. The clonal and mutational evolution spectrum of primary triple-negative breast cancers. Nature 2012;486:395–9.
5. Zhao BY, Pritchard JR, Lauffenburger DA, Hemann MT. Addressing genetic tumor heterogeneity through computationally predictive combination therapy. Cancer Discov 2014;4:166–74.
6. Wagle N, Berger MF, Davis MJ, Blumenstiel B, Defelice M, Pochanard P, et al. High-throughput detection of actionable genomic alterations in clinical tumor samples by targeted, massively parallel sequencing. Cancer Discov 2012;2:82–93.
7. Frampton GM, Fichtenholtz A, Otto GA, Wang K, Downing SR, He J, et al. Development and validation of a clinical cancer genomic profiling test based on massively parallel DNA sequencing. Nat Biotechnol 2013;31:1023–31.
8. Bamford S, Dawson E, Forbes S, Clements J, Pettett R, Dogan A, et al. The cosmic (catalogue of somatic mutations in cancer) database and website. Br J Cancer 2004;91:355–8.
9. Mardis ER. A decade's perspective on DNA sequencing technology. Nature 2011;470:198–203.
10. Kerick M, Isau M, Timmermann B, Sultmann H, Herwig R, Krobitsch S, et al. Targeted high throughput sequencing in clinical cancer settings: formaldehyde fixed-paraffin embedded (FFPE) tumor tissues, input amount and tumor heterogeneity. BMC Med Genomics 2011;4:68.
11. Lawrence MS, Stojanov P, Mermel CH, Robinson JT, Garraway LA, Golub TR, et al. Discovery and saturation analysis of cancer genes across 21 tumour types. Nature 2014;505:495–501.
12. Kandoth C, McLellan MD, Vandin F, Ye K, Niu B, Lu C, et al. Mutational landscape and significance across 12 major cancer types. Nature 2013;502:333–9.
13. Futreal A, Coin L, Marshall M, Down T, Hubbard T, Wooster R, et al. A census of human cancer genes. Nature Rev Cancer 2004;4:177–83.
14. Zack TI, Schumacher SE, Carter SL, Cherniack AD, Saksena G, Tabak B, et al. Pan-cancer patterns of somatic copy number alteration. Nat Genet 2013;45:1134–40.
15. Mao Y, Chen H, Liang H, Meric-Bernstam F, Mills GB, Chen K. CanDrA: cancer-specific driver missense mutation annotation with optimized features. PloS One 2013;8:e77945.
16. Barretina J, Caponigro G, Stransky N, Venkatesan K, Margolin AA, Kim S, et al. The cancer cell line encyclopedia enables predictive modelling of anticancer drug sensitivity. Nature 2012;483:603–7.
17. Bailey AM, Mao Y, Zeng J, Holla V, Johnson A, Brusco L, et al. Implementation of biomarker-driven cancer therapy: existing tools and remaining gaps. Discov Med 2014;17:101–14.
18. Cancer Genome Atlas Network. Comprehensive molecular characterization of human colon and rectal cancer. Nature 2012;487:330–7.
19. Palles C, Cazier JB, Howarth KM, Domingo E, Jones AM, Broderick P, et al. Germline mutations affecting the proofreading domains of POLE and POLD1 predispose to colorectal adenomas and carcinomas. Nat Genet 2013;45:136–44.
20. Walter MJ, Shen D, Ding L, Shao J, Koboldt DC, Chen K, et al. Clonal architecture of secondary acute myeloid leukemia. N Engl J Med. 2012;3661090–8.
21. Singh RR, Patel KP, Routbort MJ, Reddy NG, Barkoh BA, Handal B, et al. Clinical validation of a next-generation sequencing screen for mutational hotspots in 46 cancer-related genes. J Mol Diagn 2013;15:607–22.
22. Gutmann A. Ethics. The bioethics commission on incidental findings. Science 2013;342:1321–3.